Nanoscale

View Online
Dynamic Article Links

Cite this: *Nanoscale*, 2011, **3**, 1485

www.rsc.org/nanoscale

COMMUNICATION

Near infrared broadband emission of $In_{0.35}Ga_{0.65}As$ quantum dots on high index GaAs surfaces

Jiang Wu, Zhiming M. Wang,* Vitaliy G. Dorogan, Shibin Li, Yuriy I. Mazur and Gregory J. Salamo

Received 12th December 2010, Accepted 25th January 2011
DOI: 10.1039/c0nr00973c

Downloaded by Chengdu Library of Chinese Academy of Science on 19 October 2011
Published on 08 March 2011 on http://pubs.rsc.org | doi:10.1039/C0NR00973C

The morphology and optical properties of $In_{0.35}Ga_{0.65}As$/GaAs quantum dots (QDs) grown on (210), (311)A, (711)A, (731) and (100) substrates are investigated. QDs formed on (210) and (731) oriented substrates are grown by molecular beam epitaxy. Regular QDs are observed on (100), (311)A, and (711)A. Randomly distributed QDs and comet-shaped QDs form on (210) and (731) substrates, respectively. A high density of QDs on the order of 10^{11} cm^{-2} are obtained from (711)A. The optical measurement shows a spectrum linewidth (FWHM = 74.3 nm) of QDs on GaAs (210) three times wider than GaAs (100) substrate. Long exciton decay times, over 1 ns, are also measured by time-resolved photoluminescence technique for all samples. Our results demonstrate the potential for QDs on GaAs high index substrates for wideband applications.

Introduction

To date, self-assembled quantum dots (QDs) have attracted great attention in novel electronic and optoelectronic applications, such as low-threshold lasers, high performance infrared detectors, intermediate band solar cells, and superluminescent diodes (SLDs).[1–7] Despite great development of basic physical understanding and practical applications for QDs, there are still tremendous research efforts devoted to the study of the formation and characterization of QDs.[8–14] Among these works, high-index substrates have been of much interest because these surfaces show interesting phenomena, including strong optical anisotropies and piezoelectric effects.[15–18] Moreover, the widely studied In(Ga)As QDs grown by the Stranski–Krastanov (SK) growth mode on GaAs (100) can achieve good electronic and optical properties, at the cost of control in structural properties. On the other hand, various nanostructures, such as self-aligned quantum dot arrays, can be easily obtained by the use of high-index substrates.[19–21] These well-ordered quantum dot arrays or quantum wires grown on high index substrates open great opportunities for applications such as solid-state quantum computing and infrared photodetector. Therefore, most of the current work focuses on obtaining ordered QD arrays. Growth on high index surfaces are less studied for other applications where a random distribution of QDs is desired. For example, QD systems are proposed as one of the best candidates for broad spectrum devices due to the inhomogeneous broadening of its gain spectrum as a result of the large size distribution in self-assembled QDs.[5] However, there is no report on QDs grown on high index surfaces for SLD applications, *i.e.* a study on the increase in PL spectral width.

Hence, we investigate the morphology and optical properties of QD grown on various high index surfaces for potential applications of SLDs. In addition, most of the studies until now have focused on either GaAs (n11)A or (n11)B substrates.[15,22,23] In the present work, (210) and (731) oriented surfaces are investigated together with (100), (311)A, and (711)A surfaces and formation of QDs are observed on (210) and (731) oriented surfaces.

Experiment

The $In_{0.35}Ga_{0.65}As$ QDs are grown simultaneously on *epi*-ready GaAs substrates by a solid-source molecular beam epitaxy (MBE) 32P Riber system. Small size substrates: (100), (210), (311)A, (711) and (731)A, are mounted side by side with indium on the same molybdenum block. The substrates are carefully placed to ensure temperature variation within 10 degrees to approach identical growth conditions. During the growth, the molybdenum block is rotated to ensure flux homogeneity. The deoxidization is measured from RHEED *in situ*. To ensure complete desorption of the oxide layer, substrate temperature is increased by 20 degree above deoxide temperature and kept at this temperature for 10 min. After oxide desorption at 600 °C, a GaAs buffer layer of 500 nm is grown at substrate temperature of 580 °C with a growth rate of one monolayer (ML) per second. Sequentially, 400 nm GaAs is grown at 0.7 ML s^{-1}, followed by 50 nm $Al_{0.3}Ga_{0.7}As$ layer. The beam equivalent pressure is kept constant at $\sim 1 \times 10^{-5}$ Torr As4 beam equivalent pressure for the entire growth. The active region consists of 20 ML $In_{0.35}Ga_{0.65}As$ QDs sandwiched by 50 nm GaAs barriers. The QDs are grown at a substrate temperature of 520 °C. A second 50 nm $Al_{0.3}Ga_{0.7}As$ layer is grown after the growth of the active layers. Lastly, the final layer of 50 nm GaAs and 20 ML $In_{0.35}Ga_{0.65}As$ QDs are deposited on the surface for AFM study. The optical properties of all samples are then studied by photoluminescence (PL) technique. PL measurements are performed using the 532 nm excitation from a Nd : YAG laser with a spot diameter at the sample of 20 μm. The

Arkansas Institute of Nanoscale Materials Science and Engineering, University of Arkansas, Fayetteville, AR, 72701, USA. E-mail: zmwang@uark.edu; Fax: +479 575 4580; Tel: +479 575 4217

View Online

Downloaded by Chengdu Library of Chinese Academy of Science on 19 October 2011
Published on 08 March 2011 on http://pubs.rsc.org | doi:10.1039/C0NR00973C

time resolved PL measurements are performed using a mode-locked Ti : sapphire laser.

Results and discussion

Fig. 1 shows AFM images of $In_{0.35}Ga_{0.65}As$ QDs on (a) (100), (b) (311)A, (c) (711)A, and (d) (731) surfaces with 1 μm × 1 μm field of view. Fig. 2 shows the AFM images of QDs on (210) surface with 4 μm × 4 μm. The QDs in Fig. 1(a), the (100) substrate, have a density of 6.4×10^{10} cm^{-2} and an average height of ~8.1 nm. On the other hand, the QDs on (210), (311)A, (711)A, (731) substrates have densities of 9.4×10^{8} cm^{-2}, 6.9×10^{10} cm^{-2}, 1.6×10^{11} cm^{-2} and 6.6×10^{10} cm^{-2} and average heights of 7.3 nm, 6.4 nm, 9.0 nm and 6.7 nm. The densities of QDs on different substrates are plotted in the inset of Fig. 1(d). By depositing 20 ML $In_{0.35}Ga_{0.65}As$, QDs with high areal density are observed on (100), (311)A, (711)A and (731) oriented substrates. The highest density of QDs is observed from (711)A. The density of QDs on the (210) substrate is over an order of magnitude less than the other four substrates. As shown in Fig. 2(a), the low density of QDs on (210) is due to the fact that the $In_{0.35}Ga_{0.65}As$ prefers to nucleate into wire-shaped structures rather than form QDs. The QDs on the (210) substrate are mainly observed to form on the wire-shaped ridges. These wire-shaped structures may be related to the mesoscopic steps formed on (210) surface. The fact has been well recognized that nucleation prefers to happen at step regions, particularly ragged steps due to its active reaction.[24] In addition to the difference in areal density of QDs, the shape and size of QDs show obvious differences depending on substrate orientations as well. For example, irregular QD shapes are observed on the (711)A surface and comet-shaped QDs are formed on the (731) surface. Large nanostructures with a lateral size of about 200 nm and large size distribution are observed on (210). The large size of nanostructures can be explained by preferred nucleation sites along the mesoscopic steps. As shown in Fig. 2(b) and (c), the QDs demonstrate large size variation along the wire-shaped ridges.

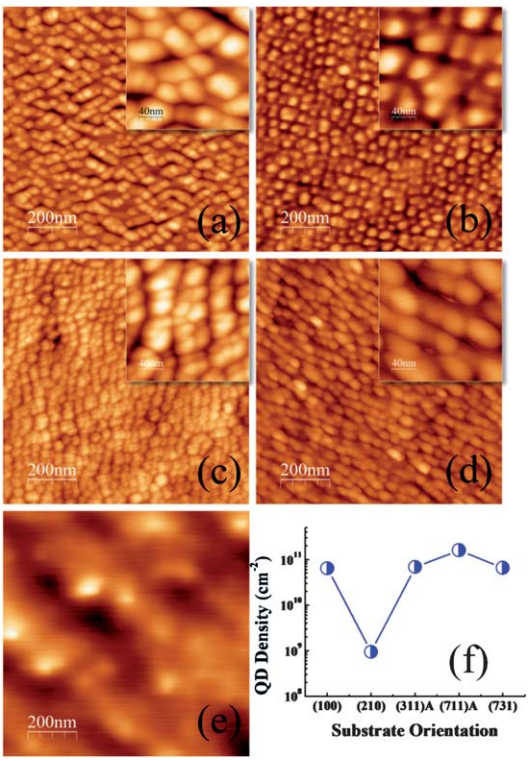

Fig. 1 (a), (b), (c), (d), and (e) are 1 × 1 $μm^2$ AFM images of $In_{0.35}Ga_{0.65}As$ QDs formed on (100), (311), (711), (731), and (210) GaAs surfaces, respectively. The insets in (a)–(d) are the magnified 200 × 200 nm^2 AFM images. (f) shows the QD density as a function of substrate orientations. The vertical scale of (a), (b), (c), and (d) is 20 nm and (e) is 30 nm. The *Z*-scale of the inset images is 15 nm.

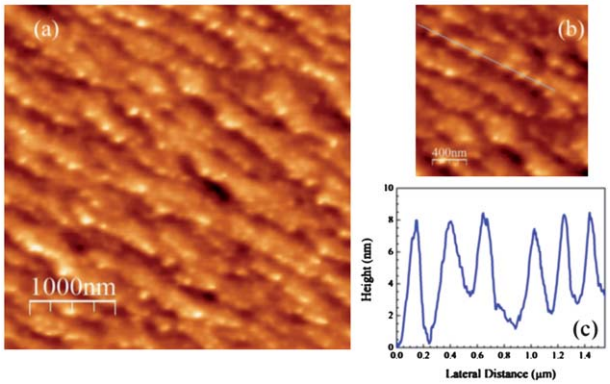

Fig. 2 (a) 4 × 4 μm AFM image of $In_{0.35}Ga_{0.65}As$ QDs on (210) surface. (b) Zoom-in AFM image of $In_{0.35}Ga_{0.65}As$ QDs on (210) surface. The line indicates the position that the cross-sectional line profile shown (c) is taken.

Normalized PL spectra at 10 K are shown in Fig. 3 for all five samples. The PL spectra are obtained under the excitation power intensity of 5 W cm^{-2} which is low enough to make broadening from excited states negligible. Additionally, PL linewidth broadening due to thermal distribution of carriers is also minimized at temperatures as low as 10 K. A redshift is observed for QDs on high index surfaces, especially the (731) surface, with reference to the (100) substrate, which may be attributed to the anisotropy of the heavy-hole bands in the different GaAs oriented surfaces.[25] Due to the anisotropy of the valance band near Γ, the hole energy levels are dependent on surface orientations and are closer to the valence band edge on high index surfaces compared with QDs on (100) surfaces. In addition, PL from QDs grown on (100), (311)A, (711)A and (731) have a similar single Gaussian shape while a non-Gaussian PL spectrum is observed for

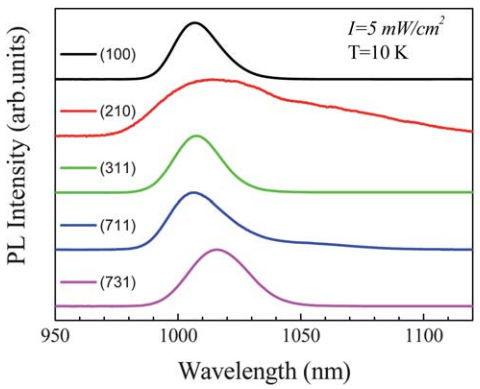

Fig. 3 Normalized PL spectra of $In_{0.35}Ga_{0.65}As$ QDs grown on high-index surfaces at 10 K. The laser excitation power is 5 mW cm^{-2}.

This journal is © The Royal Society of Chemistry 2011

View Online

Downloaded by Chengdu Library of Chinese Academy of Science on 19 October 2011
Published on 08 March 2011 on http://pubs.rsc.org | doi:10.1039/C0NR00973C

QDs on the (210) substrate. The non-Gaussian spectrum shape is caused by transitions from both the wires and the dot-like nanostructures on (210) surface. Table 1 summarizes peak positions, full width at half maximum (FWHM), and the integral PL intensity values for all samples. Narrow PL linewidth is observed for QDs on (100) and (311)A, with FWHM of ~22 nm. The broadening of the PL spectrum is mainly due to the inhomogeneous broadening of QDs. The FWHM of the PL spectrum is 74.3 nm for the (210) surface. We attribute the spectrum broadening to the randomness of the nanostructures on (210) surface. The (210) surface has asymmetric pyramids forming in two directions, [011] and [$\bar{1}$20], on the (210) surface. Such asymmetric facets may lower the degree of ordering of the surface nanostructures on GaAs (210) compared with other surfaces.[26] Moreover, the interface roughness, resulting from the mesoscopic steps, can cause significant size dispersion of wires and dot-like nanostructures on the (210) surface and further lead to a large spectral width in PL measurement. Fig. 4 shows the PL spectra of the nanostructures on (210) surface. The excitation power is 5 mW cm^{-2} and 3300 W cm^{-2}, respectively. With increasing excitation power, the FWHM and spectral lineshape remains almost the same. However, the PL spectrum undergoes a blueshift with increasing excitation power due to state-filling effects. Given that the PL spectra demonstrate similar linewidth and lineshape at both high and low excitations, the PL broadening is attributed to non-uniform surface nanostructure distribution. The wide spectrum linewidth obtained from the (210) oriented surface highlights potentials of high index substrates for wideband applications, including SLDs.

In order to obtain further information on the dependence of the optical properties on the index of the substrate, time-resolved PL spectra are measured at 10 K and plotted in Fig. 5. The PL transient decays are measured at the positions of the PL peaks. Due to the relatively long exciton lifetime, these transitions are assigned to ground state QD recombination.[27] Such an argument is also supported by the PL spectrum obtained by the low excitation power. The pump energy is 750 nm and the excitation intensity incident on the sample is 13 W cm^{-2}. The PL transient decays are mono-exponential with time constants on the order of 1 ns for all samples, as shown in the inset of Fig. 5. The difference in decay time of different surfaces can be understood by different transition rates.[28] At cryogenic temperatures, the non-radiative recombination is suppressed and the transition rate is mainly due to radioactive recombination rate

$$\tau = f^{-1}\frac{2\pi\varepsilon_0 m_0 c^3}{ne^2\omega^2} \quad (1)$$

where f is the transition oscillation strength which is expected to increase as the size of the QDs decreases; m_0 and e is the electron vacuum mass and charge, respectively; c is the speed of light in vacuum; n is the refractive index; ε_0 is the dielectric constant; and, ω is the light frequency. Consequently, the measured decay time is also proportional to the size of the QDs. Since the confinement is mainly along the growth direction, the height of the QDs is the major factor affecting the oscillation strength. The height of the QDs on different surfaces is plotted with the lifetime of the excitons, as shown in the inset of Fig. 4. Even though other effects such as strain may affect decay time, the possible correlation of height and exciton lifetime agrees well with the size effects on transition rate. Therefore, other than the slight difference in decay time introduced by difference in height, the QDs on all five substrates show similar exciton lifetimes, which demonstrates comparable optical quality for QDs grown on the (100) surface and high index surfaces.

Table 1 FWHM values, integrated PL intensity, and peak wavelength (λ_{peak}) of $In_{0.35}Ga_{0.65}As$ QDs PL spectra on all orientations

Orientation	FWHM (nm)[a]	Integrated PL	λ_{peak} (nm)
(100)	21.4	1.15×10^6	1006.9
(210)	74.3	3.57×10^5	1014.1
(311)A	22.7	1.06×10^6	1007.6
(711)A	27.9	1.14×10^6	1006.9
(731)	28.2	9.34×10^5	1016.1

[a] FWHM stands for the full width at half-maximum.

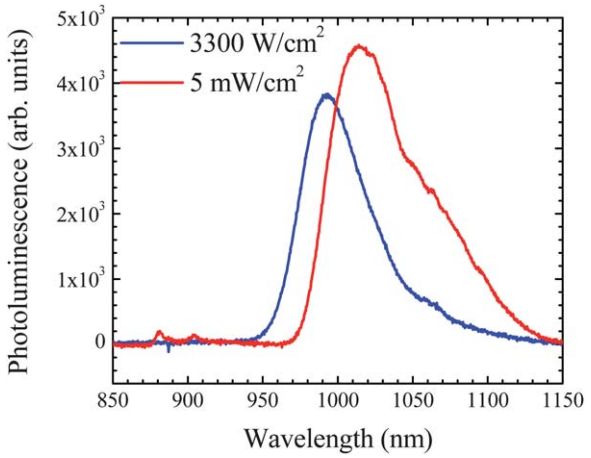

Fig. 4 Low power and high power excitation PL of nanostructures on (210) surface at 10 K.

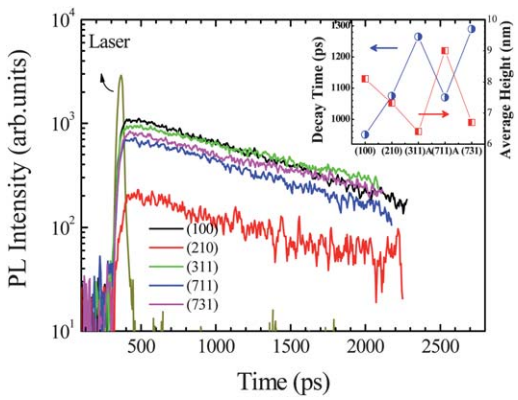

Fig. 5 PL decay transients measured at 10 K for different substrates. Inset is the exciton lifetime and QD average height as a function of substrate orientation.

Conclusion

In conclusion, the comparison of MBE grown $In_{0.35}Ga_{0.65}As$ QDs on GaAs(100) and high index surfaces is investigated. A higher density of QDs and a larger PL linewidth are observed from high index surfaces, (711)A and (210), compared to (100) surface. In addition, long exciton lifetimes of QDs on high index surfaces are revealed from time-resolved PL measurement. The AFM and PL results in this work have indicated the potential of GaAs high index surfaces for broadband emission applications.

View Online

Acknowledgements

This work was supported by the Arkansas Biosciences Institute and the MRSEC Program of NSF Grant No. (DMR-0520550).

Notes and references

1 D. L. Huffaker, G. Park, Z. Zou, O. B. Shchekin and D. G. Deppe, *Appl. Phys. Lett.*, 1998, **73**, 2564.
2 L. Jiang, S. S. Li, N. Yeh, J. Chyi, C. E. Ross and K. S. Jones, *Appl. Phys. Lett.*, 2003, **82**, 1986.
3 S. Li and J. Xia, *Phys. Rev. B: Condens. Matter*, 1997, **55**, 15434–15437.
4 K. Laouthaiwattana, O. Tangmattajittakula, S. Suraprapapicha, S. Thainoia, P. Changmuanga, S. Kanjanachuchaia, S. Ratanathamaphana and S. Panyakeow, *Sol. Energy Mater. Sol. Cells*, 2009, **93**, 746.
5 Z. Sun, D. Ding, Q. Gong, W. Zhou, B. Xu and Z. Wang, *Opt. Quant. Electron.*, 1999, **31**, 1235–1246.
6 Z. Li, J. Wu, Z. M. Wang, D. Fan, A. Guo, S. Li, S. Q. Yu, O. Manasreh and G. J. Salamo, *Nanoscale Res. Lett.*, 2010, **5**, 1079–1084.
7 S. Li, J. Xia, J. Liu, F. Yang, Z. Niu, S. Feng and H. Zheng, *J. Appl. Phys.*, 2001, **90**, 6151.
8 M. K. Yakes, C. D. Cress, J. G. Tischler and A. S. Bracker, *ACS Nano*, 2010, **4**, 3877.
9 P. Alonso-González, J. Martín-Sánchez, Y. González, B. Alén, D. Fuster and L. González, *Cryst. Growth Des.*, 2009, **9**, 2525–2528.
10 C. Heyn, A. Stemmann, T. Köppen, C. Strelow, T. Kipp, M. Grave, S. Mendach and W. Hansen, *Appl. Phys. Lett.*, 2009, **94**, 183113.
11 J. Lee, Z. M. Wang, V. G. Dorogan, Y. I. Mazur and G. J. Salamo, *IEEE Transactions on Nanotechnology*, 2009.
12 B. Liang, A. Lin, N. Pavarelli, C. Reyner, J. Tatebayashi, K. Nunna, J. He, T. J. Ochalski, G. Huyet and D. L. Huffaker, *Nanotechnology*, 2009, **20**, 455604.
13 V. G. Dorogan, Y. I. Mazur, J. H. Lee, Z. M. Wang, M. E. Ware and G. J. Salamo, *J. Appl. Phys.*, 2008, **104**, 104303.
14 K. A. Sablon, J. H. Lee, Z. M. Wang, J. H. Shultz and G. J. Salamo, *Appl. Phys. Lett.*, 2008, **92**, 203106.
15 L. Wang, M. Li, M. Xiong and L. Zhao, *Nanoscale Res. Lett.*, 2009, **4**, 689–693.
16 J. S. Kim, M. S. Jeong, C. C. Byeon, D. Ko, J. Lee, J. S. Kim, I. Kim and N. Koguchi, *Appl. Phys. Lett.*, 2006, **88**, 241911.
17 V. R. Yazdanpanah, Z. M. Wang and G. J. Salamo, *Appl. Phys. Lett.*, 2003, **82**, 1766.
18 Y. Z. Xie, V. P. Kunets, Z. M. Wang, V. G. Dorogan, Y. I. Mazur, J. Wu and G. J. Salamo, *Nano-Micro Lett.*, 2009, **1**, 1–3.
19 Z. M. Wang, S. Seydmohamadi, J. H. Lee and G. J. Salamo, *Appl. Phys. Lett.*, 2004, **85**, 5031.
20 B. L. Liang, Z. M. Wang, K. A. Sablon, Y. I. Mazur and G. J. Salamo, *Nanoscale Res. Lett.*, 2007, **2**, 609–613.
21 Z. Ma, T. Holden, Z. M. Wang, G. J. Salamo, P. Yu and S. Mao, *Appl. Phys. A: Mater. Sci. Process.*, 2009, **96**, 271.
22 S. Sanguinetti, M. Gurioli and M. Henini, *Microelectron. J.*, 2002, **33**, 583–588.
23 B. L. Liang, Z. M. Wang, Y. I. Mazur, V. V. Strelchuck, K. Holmes, J. H. Lee and G. J. Salamo, *Nanotechnology*, 2006, **17**, 2736–2740.
24 R. Nötzel, D. Eissler, M. Hohenstein and K. Ploog, *J. Appl. Phys.*, 1993, **74**, 431.
25 L. Shu-Shen and X. Jian-Bai, *Chin. Phys.*, 2007, **16**, 1–5.
26 R. Nötzel, L. Däweritz and K. Ploog, *Phys. Rev. B: Condens. Matter*, 1992, **46**, 4736.
27 Y. I. Mazur, Z. Y. Abu Waar, T. D. Mishima, J. H. Lee, G. G. Tarasov, B. L. Liang, V. G. Dorogan, M. E. Ware, Z. M. Wang, M. B. Johnson and G. J. Salamo, *J. Appl. Phys.*, 2008, **104**, 044310.
28 J. Bellessa, V. Voliotis, R. Grousson, X. Wang, M. Ogura and H. Matsuhata, *Phys. Rev. B: Condens. Matter*, 1998, **58**, 9933–9940.

Downloaded by Chengdu Library of Chinese Academy of Science on 19 October 2011
Published on 08 March 2011 on http://pubs.rsc.org | doi:10.1039/C0NR00973C

 This journal is © The Royal Society of Chemistry 2011